Fundamental Investigation of Diesel Spray-Spray Interaction for Cluster-Hole Nozzles

M. Gauding[1*], A. Pawlowski[2], C.Felsch[1], B. Sonntag[1], R. Kneer[2] and N. Peters[1]
[1]Institut für Technische Verbrennung
[2]Institut für Wärme- und Stoffübertragung
RWTH Aachen University
52056 Aachen, Germany

Abstract

Nozzles with more and smaller orifices have contributed significantly to the improvement of Diesel engine performance and emissions in recent years. However, for equispaced orifice configurations, minimal or no improvement is recorded for when the number of holes is increased above a certain threshold. This is considered to be primarily due to an increased spray-spray interaction for an increased number of holes. One way to avoid interference between adjacent sprays, enhance engine performance, and reduce emissions by the usage of more sprays per nozzle is to abandon the equispaced design and to cluster/group the orifices. The benefits of such an arrangement of nozzle holes are yet to be fully explored. In this study, sprays from such nozzles are investigated with Schlieren photography and Phase-Doppler Anemometry (PDA) in a pressurized chamber at Diesel engine-like conditions of 800 K ambient temperature and 50 bar ambient pressure. Different geometric arrangements of the clustered orifices are compared with the conventional hole arrangement for nozzles of the same flow number. The comparisons include liquid and gaseous spray penetration, as well as radial velocity profiles. In addition to the experimental measurements, numerical simulations are carried out to compliment experimental observations. The commonly used discrete droplet model (DDM) is applied in the numerical simulations. The simulations provide insight into the interaction between adjacent sprays in regard to the mixture formation process and subsequent combustion.

Introduction

Recent advancements in manufacturing nozzles with small orifices have led to increasing research efforts regarding their application in Diesel engines. Pickett and Siebers [1], for example, investigated the influence of the orifice diameter on soot formation in Diesel combustion for micro-orifice nozzles. They found that a reduction in orifice diameter improves mixing and thus results in a reduced soot formation. In Diesel engines, a reduction of orifice diameter leads to an increased number of orifices. This is due to the necessity to deliver a defined fuel quantity in a given time at a given rail pressure. However, for equispaced orifice configurations, Benajes et al., among others, observed no improvement when the number of holes is increased above a certain threshold [2]. They considered this to be primarily due to an increased spray-spray interaction for an increased number of holes. One way to avoid interference between adjacent sprays, enhance engine performance, and reduce emissions by the usage of more sprays per nozzle is to abandon the equispaced design and to cluster/group the orifices, cf. Nishida et al. [3]. Nevertheless, the benefits of such an arrangement of nozzle holes are yet to be fully explored.

In this study, the sprays from different cluster nozzles are investigated in a pressurized vessel under thermodynamic conditions relevant for Diesel engines. The different cluster nozzle arrangements include variations of the included spray angle. For comparison purposes, a spray from a conventional nozzle is investigated, too. This paper answers some fundamental questions about the interaction of clustered sprays. For the macroscopic behavior of the sprays, experimental visualization techniques are employed. A defocused laser light sheet is used to detect the liquid phase of the spray. The vapor phase is detected with a simple Schlieren technique. Furthermore, the sprays are investigated using Phase-Doppler Anemometry to simultaneously record droplet velocities and sizes for the first time, as no comparable Phase-Doppler data from sprays of clustered orifices have been found in the literature. In addition to the experimental measurements, numerical simulations are carried out to compliment experimental observations.

Experimental and Numerical Methods

PRESSURIZED CHAMBER The ambient conditions in the pressurized vessel were set at a temperature of 800 K and a pressure of 50 bar for all investigations. A continuous air flow of about 25 kg/h delivered by a compressor is

*Michael Gauding

heated electrically to the desired temperature before entering the chamber. As the fluid in the chamber is air, combustion takes place after injection. However, for the scope of this investigation, the subsequent combustion processes was not studied in detail. The chamber can be configured according to the needs of the desired investigation. Several test sections with three and four windows can be combined with a variety of heads and heaters to allow for the optical access necessary for the specific measurement task.

INVESTIGATED NOZZLES Table 1 documents the three nozzles that were investigated with visualizations and PDA. For comparability, all three nozzles have identical flow numbers of 168. At a pressure difference of Δp = 100 bar, a fuel volume of 168 cm^3 flows through the nozzles within 30 s. The KS-factor of all nozzles is 1.3. The sprays, respectively the cluster axes, are located on a cone with a full opening angle of 148°. The nozzle design is the so-called "Combined Nozzle Layout" (CNL) with a midi-sac hole. The nozzles were investigated using a "short" energizing time of 630 µs for 600 and 900 bar rail pressure and 835 µs for 1350 bar rail pressure. To obtain PDA results, a "long" energizing time was also investigated, using 3.5 ms independent of the rail pressure. For optical accessibility, nozzle configurations with three clusters were chosen for this investigation. Each cluster consists of two orifices. The distance between the orifices in each cluster is 0.6 mm. The included angle between the cluster sprays is positive, the sprays are thus diverging. Cluster nozzles with one orifice circle (see Fig. 1 for details on the cluster orientation) were employed. A spray from a conventional three-hole/three-orifice nozzle was additionally investigated for comparison purposes.

Table 1. Nozzle properties.

Number of orifices/ number of clusters	Angle between cluster sprays	Orifice diameter
6/3	+10°	93 µm
6/3	+20°	93 µm
3/0 (conventional three-hole nozzle)	-	131 µm

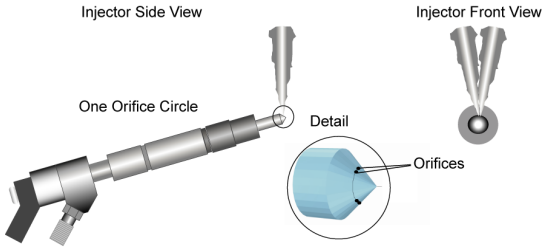

Figure 1. Sketch of orifice orientation for the investigated cluster nozzles

VISUALIZATION TECHNIQUES Visualizations are a comparably simple yet powerful tool to perform phenomenological investigations of spray processes. The chamber configuration for this investigation employs a test section with four window openings at a 90° spacing (see Fig. 2, left). Light from a defocused laser light sheet is used to detect the envelope of the liquid phase. A window in the chamber head is employed for illumination. Only droplets scatter the light, whereas the light scattering by ambient gas and fuel vapor is negligible. To ensure a uniform illumination of the sprays in the cluster, an additional window in the chamber head is used.

A backlight technique was used to quasi-simultaneously detect the envelope of both the liquid and vapor phase. Settles [4] called such an approach a "Large Colored Grid Background Distortion" technique and classified it as a simple Schlieren method, with the schlieren cutoff being in the background. This technique detects the refractive index gradients caused by the presence of fuel. It requires the light source, the object, and the detector to be aligned on a straight line. Therefore, the cluster configuration had to be mounted opposite to the camera, using a window in the injector holder for illumination. The conventional nozzle was mounted in one of the two window openings perpendicular to the one used for the camera. Typically, 20 images per time step are recorded. The image recording is completely automatized based on the DaVis software from LaVision GmbH, Germany.

An automatic image processing tool based on Matlab was developed to extract information about the penetration length and cone angle from the images. The liquid phase is extracted from the scattering light images using a threshold value defined for each image by Otsu's method [5]. The schlieren caused by the fuel in the backlight image exhibit small structures with steep intensity gradients. They are detected from the schlieren images with an edge filter based on Canny's method [6]. The resulting binary images are closed and filled. From this, selecting the largest region reliably delivers the spray envelope in the images.

PHASE-DOPPLER ANEMOMETRY The integral information gained by visualizations is supplemented by Phase-Doppler Anemometry (PDA) measurements. The PDA uses an Ar+-laser as the light source to create a small measurement volume. The PDA system can then determine the velocity and the diameter of single particles crossing the measurement volume from the light they scatter. For a detailed description of the technique see, for example, Albrecht et al. [7]. This technique has its difficulties when there is more than one particle in the measurement volume; therefore it cannot be applied to the dense part of a Diesel spray, but is restricted to the area around the stationary penetration length [7]. A typical distance from the orifice to the measurement volume is 35 mm. The setup at the

pressurized chamber is shown in Fig. 2, right. The same injector holder which is used for the visualizations is also used for PDA. In order to minimize the sensitivity to the temperature-depending refractive index of the fuel, the detector probes are positioned 65° off-axis. The size of the measurement volume is about 100 µm in diameter. At each radial position the data of 100,000 droplets or 330 injections were recorded.

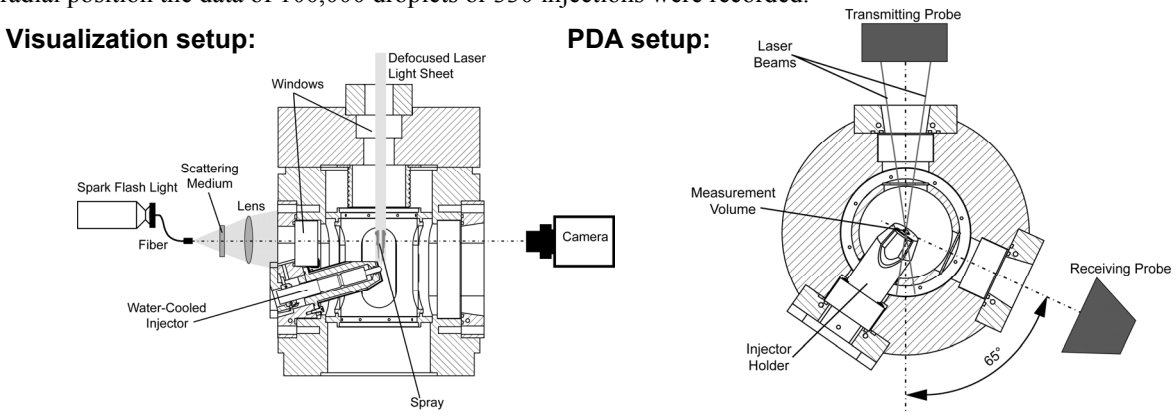

Figure 2. Left: Sketch of the visualization setup in the chamber with four window openings – side view; Right: Sketch of the PDA setup in the chamber with three window openings – top view

NUMERICAL TECHNIQUES The simulation of the spray chamber was performed by AC-FluX (formerly known as GMTEC), a flow solver based on Finite Volume methods that employs unstructured, mostly hexahedral meshes. AC-FluX solves for the partial differential equations for continuity, the Navier-Stokes equations, an equation for the total enthalpy, and two equations to account for the turbulence (k-ε-model). AC-FluX is documented by Ewald et al. [8].

The liquid phase is modeled using the discrete droplet model (DDM), which approximates the spray by a Monte-Carlo simulation. Since the spray consists of a large number of droplets, only the behavior of a representative subset of all droplets (called parcels) is calculated in detail. The gas phase and the liquid phase are coupled through source terms in the governing equations for the gas phase. A detailed description of the spray modeling in AC-FluX can be found in Spiekermann et al. [9].

The spray model parameters are always subject to adjustment and were adapted such that the experimental liquid and gaseous spray penetration were reproduced. The parameters used in this work are within the recommended parameter range proposed by Weber et al. [10]. The spray model parameters are kept constant for each nozzle.

The surrogate fuel for Diesel used in the simulation is a mixture of 30 % α-methylnaphthalene and 70 % n-decane by liquid volume, as proposed within the IDEA-EFFECT program. The injection rate is taken from rate measurements using a Bosch-type flow bench.

Results and Discussion

VISUALIZATION RESULTS First, some characteristic single images from the spray with an angle of 20° between the cluster sprays are discussed. The left image in Fig. 3 shows the light scattered by the fuel jet 1 ms after energizing the injector. The rail pressure for this injection was set to 900 bar, the total energizing time was 630 µs. Only the liquid phase is visible in the image, as the vapor phase scatters almost no light. The right image in Fig. 3 shows a back-lit schlieren image of the same injection event 15 µs later. The vapor phase is indicated by the presence of schlieren downstream of the liquid phase. The scattering light indicates that the liquid phases of the two sprays are clearly separated. The included angle between the two spray plumes equals approximately the included angle of the orifices. Similar conclusions can be drawn from the schlieren image. However, the schlieren in between the two spray axes indicate that the two spray plumes are not completely separated but are connected by evaporated fuel. It is important to note that such a partial separation was not observed for the nozzle with an angle of 10° between the cluster sprays. In this case, both the liquid and the vapor phase of both cluster sprays merged 10 mm downstream of the nozzle.

A comparison of the vapor phase penetration of all three investigated nozzles is shown in Fig. 4. The conventional nozzle penetrates faster than the cluster nozzles. This is not only true for the vapor phase, but also for the liquid phase (not shown here for brevity). This can be attributed to the larger dispersion of the cluster sprays. It is remarkable that the cluster nozzles behave very similar in terms of vapor penetration. Due to the smaller dispersion and a much stronger interaction between the jets, the 10°-cluster nozzle could be expected to deliver a faster penetration than the 20°-cluster configurations. However, this is not observed in the experiment. This is consistent with

Nishida et al. [3], who showed that at an angle of 10° between the cluster sprays, the spray penetration is similar to the penetration of an individual spray from the cluster. Thus, at angles of 10° and above in a cluster spray, no effect seems to exist that increases the cluster penetration length above the one of an individual spray of the cluster. An increasing penetration length can be found for angles of 5° and smaller, according to [3]. Although the gas phase of the 20°-cluster configuration is interacting, the liquid phases of these cluster sprays are separated. It should also be noted here that the spray penetration of the conventional nozzle correlates well with the Naber-Siebers model [11].

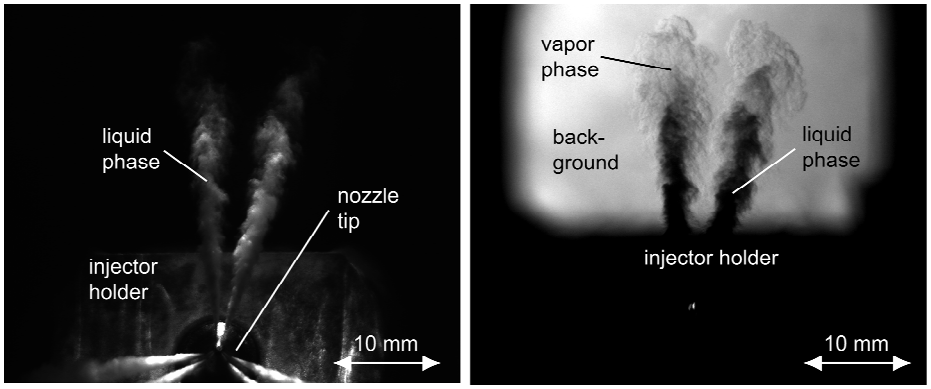

Figure 3. Scattering light (left) and schlieren (right, 15 µs later) image of the spray from the nozzle with 20° between the cluster sprays, 1 ms after energizing the injector

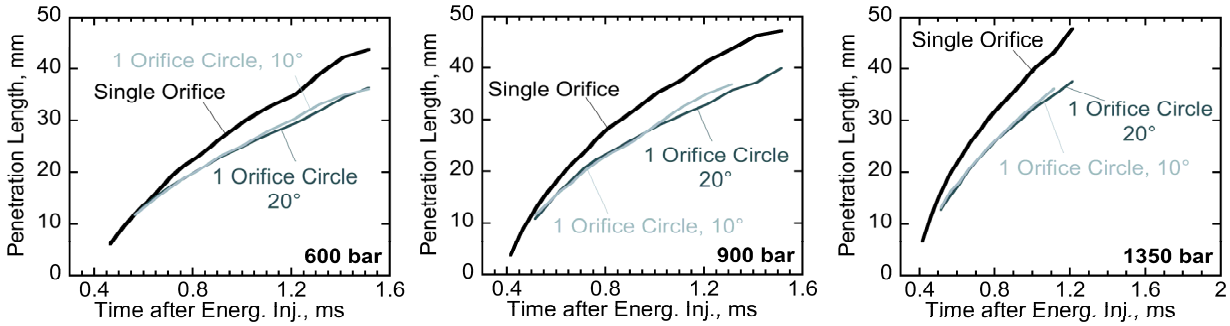

Figure 4. Comparison of vapor phase penetration behavior of all investigated nozzles; each graph represents one rail pressure

PDA RESULTS PDA measurements deliver the velocities, as well as the diameters of the particles crossing the measurement volume. Due to the large optical density of the conventional three-hole nozzle, no statistically reliable PDA data could be captured closer than 35 mm to the orifice. This issue is especially significant at high rail pressures [7]. In order to ensure comparable measurements, the axial position of the measurement volume was kept constant at 35 mm. There, the low volatility of the Diesel fuel enabled meaningful measurements at the same distance for all nozzles.

The PDA is effectively a single particle counter; for this reason only the long energizing time was investigated, as it helps to collect more droplets per injection and therefore reduces the number of injections necessary to get satisfying statistics. In each measurement point, data was collected until either 100,000 droplets were recorded or until a maximum of 330 injection events was reached. The latter criterion applied only at the spray border, where the number density of the droplets is significantly reduced.

Figure 5, left, shows the radial distribution of the measured axial velocity for different rail pressures for the spray from the conventional three-hole nozzle. A higher rail pressure results in a higher average velocity. This is particularly true for the center position of the spray, whereas at the border the increase in spray velocity is comparably small. The velocity gradient in the spray increases.

For the cluster nozzles, not one but two spray center points needed to be identified. This was done by applying the abovementioned procedure twice. In steps of 1 mm, the measurement system was traversed from the center of one spray to the center of the other spray and then towards the spray border in the same direction. The distance between the spray centers is summarized in Table 2. The spatial origin of all following graphs is the center point of the first spray. As can be seen in Table 2, the distance between the spray centers is considerably smaller for the nozzle

with 10° between the sprays than for the nozzles with 20°. The rail pressure has an influence but exhibits no clear trend. From geometric considerations, one would expect at a distance of 35 mm from the orifice a gap of about 6 mm between the spray centers for the 10° nozzle and 12 mm for the 20° nozzles. The deviation from the geometric expectations is significantly higher for the nozzle with 10° between the sprays than for the one with 20°.

Figure 5, center, deals with the sprays from the cluster nozzle with 10° between the cluster sprays. The velocity distribution is very different compared to the distribution from the conventional orifice. The two velocity maxima can hardly be recognized, as the sprays from this nozzle produce a velocity plateau with very small gradients that is 3 to 5 mm wide. At 1350 bar, this plateau is considerably smaller than for 600 and 900 bar, indicating an increase in spray-spray interaction with rail pressure for this nozzle. For sprays from cluster nozzles, a higher rail pressure results in a higher average velocity, too. The velocity plateau shifts to a higher level, whereas at the border of the sprays the increase in spray velocity is comparably small. The velocity gradient increases, which is similar to what is observed in the sprays from conventional nozzles. However, the velocity magnitude on the spray axis is about 20 % lower than in the spray from the conventional nozzle.

Figure 5, right, shows the radial distribution of the measured axial velocity for the sprays from the nozzle with 20° between the cluster sprays. The velocity distributions exhibit very different features to the one in the sprays from the conventional nozzle and the orifice circle with 10° between the cluster sprays, as the two velocity maxima are clearly separated from each other. A clear velocity minimum is visible in between the sprays around 5 mm from both spray centers, independent of the rail pressure. The velocity distributions have no plateau but are similar to two conventional sprays just next to each other. For each rail pressure, both velocity maxima have a very similar magnitude. However, as for the other nozzles, an increase in rail pressure results in higher velocities close to the spray center. The velocity change at the spray borders is comparably small, so the velocity gradients in the spray increase with the rail pressure. The velocity magnitude in the two spray centers shows similar values than for the sprays from the 10°-cluster nozzle. In quasi-steady state, no differences/instabilities between the sprays are noticed.

For brevity, no data on the diameter distribution is shown. The Sauter diameter for all cluster nozzles (5-9 µm) is considerably smaller than for the conventional nozzle (8-15 µm). This is probably due to the smaller orifice diameter of the cluster nozzles compared to the conventional nozzle.

In summary, the PDA results confirm the finding of the visualizations that the liquid phases of the sprays from the 20°-cluster configurations are separated, whereas the sprays from the 10°-cluster configurations merge. The velocity magnitude in the sprays from all the investigated cluster nozzles is about 20 % smaller than the velocities measured in the sprays from the conventional nozzle. This is in agreement with the comparably slower penetration of the sprays from the cluster nozzles. As the spray penetration depends on the orifice diameter, the reason for the slower penetration is probably the smaller orifice diameter of the cluster nozzles and the therefore larger dimensionless distance based on the single orifice diameter.

Table 2. Rail pressure dependence of the distance between the spray centers for the cluster nozzles.

Nozzle	600 bar	900 bar	1350 bar
+10°	3.5 mm	4.0 mm	3.0 mm
+20°	10.5 mm	9.0 mm	10.0 mm

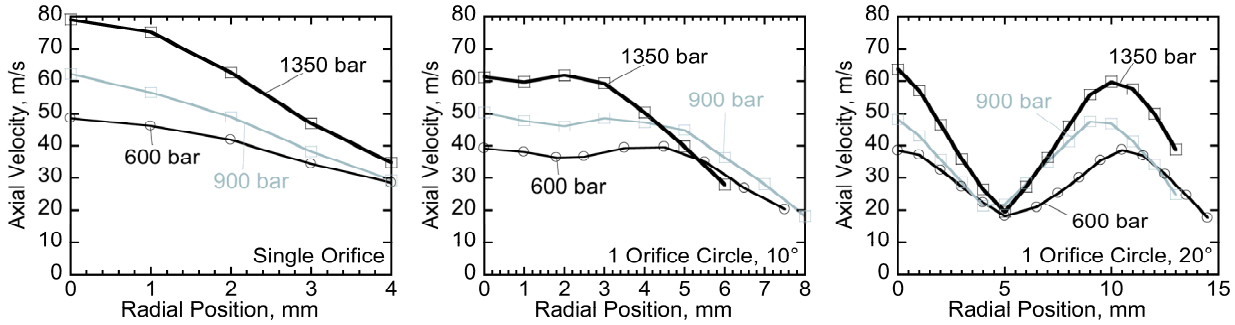

Figure 5. Radial distribution of axial velocity for different rail pressures for the spray from the conventional three-hole nozzle (left) and the cluster nozzles with 10° (center) and 20° (right) between the cluster sprays, averaged from 1.5 to 2.5 ms after energizing the injector

NUMERICAL RESULTS In the CFD simulations, the spray chamber was represented by a cylinder that was meshed by means of an O-grid topology. The finest mesh resolution was in the area around the nozzle, with a cell

size of approximately 0.6 mm in each direction. The radius of the computational domain was 50.0 mm and the height was 90.0 mm. The total mesh resolution was 235,340 cells. Figure 6, left, depicts the computational mesh. 20000 parcels per nozzle were used in the simulations. Figure 6 further deals with the 20°-cluster configuration with 900 bar rail pressure and an energizing time of 630 µs. It shows the temperature distribution (center) and the fuel mass fraction distribution (right) in the injector cut plane 1.05 ms after start of injection. The liquid phase is illustrated, too. When adjusting the spray model parameters such that experimental and numerical liquid and vapor penetration length match, the DDM model is able to reasonably capture the mixture formation process [9]. The simulation results support the experimental observations. The liquid phases of the cluster sprays are separated, the vapor phases merge.

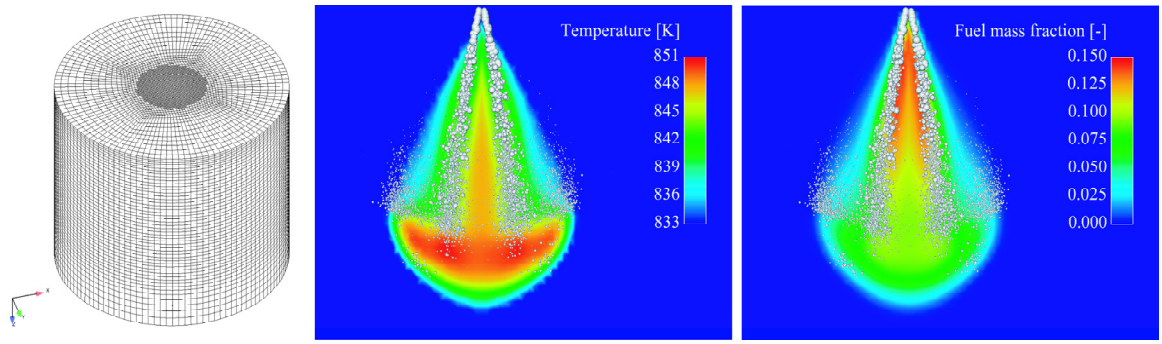

Figure 6. Computational mesh (left), as well as temperature distribution (center) and fuel mass fraction distribution (right) in the injector cut plane 1.05 ms after start of injection

Summary and Conclusions

The sprays from a set of nozzles with clustered orifices were investigated and compared to a spray from a conventional nozzle. Visualization techniques and Phase-Doppler Anemometry were used to characterize the sprays from such nozzles. A significant effect of the cluster geometry on spray formation was noticed. Direct spray-spray interaction was found in all cases, with varying intensity depending on the included angle of the orifices within a cluster. The sprays from all investigated cluster nozzles penetrated significantly slower and showed smaller axial drop velocities than those of the conventional nozzle. Numerical simulations carried out with the DDM model complimented the experimental investigations.

Acknowledgments

The authors would like to thank General Motors Corporation for the financial support in the framework of the "Corporate Research Lab (CRL) at RWTH Aachen University" and the other members of the CRL for their support and contribution.

References

1. Pickett, L.M., and Siebers, D.L., *Proc. Comb. Inst.* 29:655-662 (2003).
2. Benajes, J., Molina, S., De Rudder, K., Maroteaux, D., Ben Hadj Hamouda, H., *I MECH E Part D: Journal of Automobile Engineering*, 220:1807-1817 (2006).
3. Nishida, K., Nomura, S., Yuhei, M., ICLASS-2006, 10th International Congress on Liquid Atomization and Spray Systems, Kyoto, Japan, 2006.
4. Settles, G.S., *Schlieren and Shadowgraph Techniques*, Springer, 2006.
5. Otsu, N., *IEEE Transactions on Systems, Man, and Cybernetics*, 9:62-66 (1979).
6. Canny, J., *IEEE Transactions on Pattern Analysis and Machine Intelligence*, 8:679-698 (1986).
7. Albrecht, H.E., Borys, M., Damaschke, N., Tropea, C., *Laser Doppler and Phase Doppler Measurement Techniques*, Springer, 2002.
8. Ewald, J., Freikamp, F., Paczko, G., Weber, J., Haworth, D.C., Peters, N., "GMTEC: GMTEC Developer's Manual". Technical report, Advanced Combustion GmbH, 2003.
9. Spiekermann, P., Jerzembeck, S., Felsch, C., Vogel, S., Gauding, M., Peters, N., *Atomization and Sprays* 19:357-386 (2009).
10. Weber, J., Spiekermann, P., Peters, N., SAE 2005-01-2099, 2005
11. Naber, J.D., and Siebers, D.L., SAE 960034, 1996